

Acyclic butyl nucleic acid (BuNA): a novel scaffold for A-switch†

Cite this: *RSC Advances*, 2013, 3, 19330

Vipin Kumar and Venkitasamy Kesavan*

The construction of an A-switch, derived from the artificial nucleic acid called acyclic Butyl Nucleic Acid (BuNA) was accomplished. The phosphoramidite building blocks of (S)-BuNA were synthesized from (R)-aspartic acid. To demonstrate its use as an A-switch, a stretch of polyadenine nucleotides of (S)-BuNA was studied by circular dichroism (CD) and ultraviolet (UV) spectroscopy under neutral and acidic conditions. Acid–base titration revealed two state transitions at pH 4.8 and highly pH-dependent structural conformation reversibility. Thermal melting (T_m) studies suggest that at neutral pH, poly BuNA(A) is a weakly organized single strand, while at low pH it adopts a highly organized and rigid structure. Furthermore, MALDI-TOF-MS data revealed intermolecular interactions which led to the formation of an A-motif composed of a double helical structure. Since BuNA does not suffer from depurination under acidic conditions, this allowed us to determine the thermodynamic parameters of the A-motif. This is the first report of the construction of an A-switch using artificial nucleic acids.

Received 15th March 2013,
Accepted 2nd August 2013

DOI: 10.1039/c3ra41255e

www.rsc.org/advances

Introduction

The growing field of DNA technology requires new chemically modified nucleic acid analogues that can perform advanced and superior functions with greater chemical stability.¹ Artificial nucleotide analogues have been widely explored in order to modulate the nucleic acids, which make them promising building blocks for constructing molecular devices.² These molecular devices are made up of unusual structures, involving non-Watson–Crick base pairing such as in i-motif, G-quadruplex and A-motif.³ In order to modulate the properties of these molecular devices with superior functions, researchers have investigated various analogues of natural nucleotides like Unlocked Nucleic Acid (UNA),⁴ Locked Nucleic Acid (LNA),⁵ Peptide Nucleic Acid (PNA),⁶ methylphosphonate,⁷ phosphoramidite,⁷ phosphorothioate⁸ and 3'-S-phosphorothiolate,⁹ which have been incorporated into nucleic acid structures. In addition, DNA has been used for construction of the nanomechanical devices based on the B-Z conformational transition.¹⁰

Chemical modification of nucleic acids can be achieved by modifying the sugar-phosphate backbone or the nucleobase moieties.¹¹ Researchers have investigated various artificial nucleic acid systems containing nondeoxyribose,¹² acyclic backbones¹³ and polypeptide backbones.¹⁴ Artificial nucleic

acids containing negatively charged phosphodiester linkages have an advantage over a peptide backbone as they facilitate the solubility in aqueous medium.

Since acyclic nucleotides are structurally simplified¹⁵ so the chemical synthesis of their phosphoramidite building blocks can be achieved by rather simple organic transformations. Glycol Nucleic Acid (GNA)^{16a} reported by Eric Meggers was used for constructing two mirror image 4-Helix Junctions.^{16b} This report suggests that acyclic nucleic acid can be used for constructing nanostructures. On similar lines, Threoninol Nucleic Acid (aTNA)^{17a} and Serinol Nucleic Acid (SNA)^{17b} have been demonstrated as C-3 scaffold-based acyclic nucleic acids, which adopt A-form and B-form-like helical structures respectively. Furthermore, aTNA has been demonstrated to be an effective scaffold for constructing photo switches.¹⁸ In addition, by using artificial nucleic acid building blocks, it might be possible to create molecular devices with new chemical and physical properties which are not observed in DNA/RNA-based devices.

The molecular properties of poly r(A) at low pH were studied by Fresco and Klemperer.¹⁹ In 1961, Rich *et al.* investigated the organization of adenine moieties at low pH in a duplex of poly r(A) by X-ray studies.²⁰ These studies revealed that poly r(A) adopts a parallel right handed double stranded helical structure at low pH and strands are held together by Hoogsteen base-pairing ($A^+ \cdot A^+$) and salt bridges between the protonated N1 of adenine and the phosphate backbone. Recent reports illustrated the conformational changes of poly d(A)₁₅ at low pH and its use as a DNA-based pH sensor.²¹ Therefore, low pH is essential for poly d(A) to act as an A-switch but undermines the chemical stability of the

Chemical Biology Laboratory, Department of Biotechnology, Indian Institute of Technology Madras (IITM), Chennai 600036, India. E-mail: vkesavan@iitm.ac.in; Tel: +91-44-22574124

† Electronic supplementary information (ESI) available: Synthesis, characterization, NMR spectra, MALDI-TOF-MS and additional figures are provided. See DOI: 10.1039/c3ra41255e

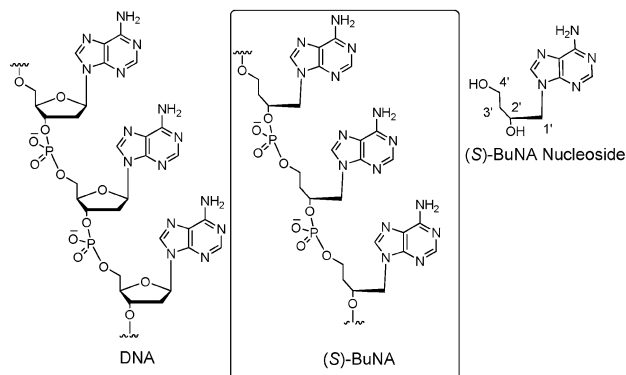


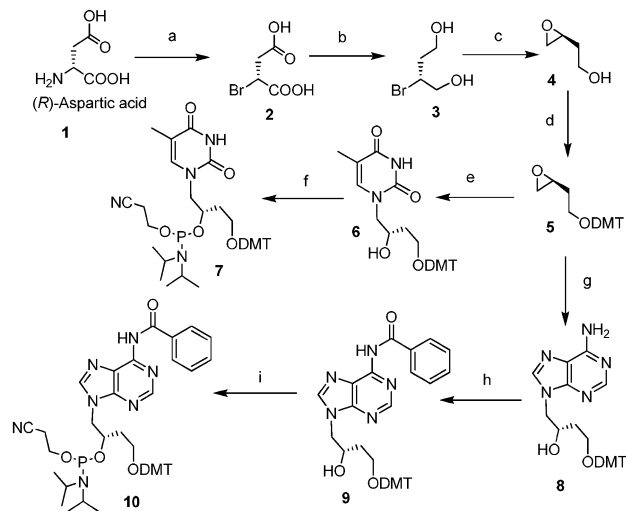
Fig. 1 Chemical structures of DNA, (S)-BuNA and (S)-BuNA nucleoside.

N-glycosidic bond of purines under the same conditions.²² G-quadruplexes and i-switches have been developed from PNA, but this system cannot be used for constructing an A-switch due to its neutral peptide backbone. Hence, it is vital to explore new artificial nucleic acids, which are chemically and enzymatically more stable, in order to construct molecular devices with superior functions. Recently, we have investigated the pairing properties of acyclic Butyl Nucleic Acid (BuNA) and its incorporation in to DNA strands.²³ Herein, we report the construction of a functional A-motif from acyclic Butyl nucleic acid (BuNA) (Fig. 1) which behaves as an A-switch by acid–base changes.

Result and discussion

Design and synthesis of (S)-BuNA

The design of the acyclic scaffold was based on the six-bonds-per-backbone unit^{13c} of vicinal phosphodiester groups similar to DNA or RNA, which may enable conventional Watson–Crick or Hoogsteen base-pairing as in unmodified nucleic acids (Fig. 1). Accordingly, (*R*)-aspartic acid **1** was converted into bromosuccinic acid **2** by the diazotization reaction in the presence of sodium bromide. Compound **2** was reduced by borane dimethyl sulphide in dry THF at 0 °C to give corresponding bromodiol **3**. Treatment of **3** with cesium carbonate in dry dichloromethane afforded the epoxide **4** in 65% yield. Preparation of DMT-epoxide **5** was achieved by treatment of **4** with DMT-Cl in the presence of triethylamine in 60% yield. DMT-epoxide underwent ring opening with the respective nucleobases in the presence of 0.3 equivalent of NaH to afford DMT-alcohols **6** and **8** (Scheme 1). Heteronuclear multiple-bond correlation (HMBC) spectroscopy was used for the confirmation of regioselectivity of nucleobase *N*-alkylation (Fig. S4, ESI†). To avoid side reactions in the phosphitylation step, the exocyclic amine of adenine was protected by the benzoyl group to give **9** in 67% yield. Phosphitylation of DMT-alcohols was carried out using 1.5 equivalents *N,N,N',N'*-tetraisopropylphosphordiamidite and 0.5 equivalent diisopropyl ammonium tetrazolide in anhydrous dichloromethane, yielding the phosphoramidite build-



Scheme 1 Synthesis of phosphoramidite building blocks of (S)-BuNA. (a) HNO_2/HBr , 60% yield. (b) $\text{Me}_2\text{S}\cdot\text{BH}_3$, THF, 87%. (c) Cs_2CO_3 , CH_2Cl_2 , 65%. (d) DMT-Cl, triethylamine, CH_2Cl_2 , 60%. (e) Thymine, 0.3 equiv. NaH, dry DMF, 110 °C, 45%. (f) 2-Cyanoethyl *N,N,N',N'*-tetraisopropylphosphordiamidite, diisopropyl ammonium tetrazolide, CH_2Cl_2 , 73%. (g) Adenine, 0.3 equiv. NaH, dry DMF, 110 °C, 45%. (h) 3 equiv. TMS-Cl, benzoyl chloride, anhydrous pyridine, 60%. (i) 2-Cyanoethyl *N,N,N',N'*-tetraisopropylphosphordiamidite, diisopropyl ammonium tetrazolide, CH_2Cl_2 , 67%.

ing blocks of A and T in 63% and 73% yield respectively.²³ Synthesis of oligonucleotides was carried out using an automated solid-phase oligonucleotide synthesizer by standard protocol (Table 1). Purification of oligonucleotides was carried out by preparative denaturing polyacrylamide gel electrophoresis (PAGE) and product identity was confirmed by MALDI-TOF-MS (Table S5, ESI†).

Incorporation of (S)-BuNA nucleotides in to DNA strand and pairing properties of poly BuNA (A) and poly BuNA (T)

Prior to demonstrating the use of BuNA as molecular switch, it is important to study the effect of (S)-BuNA nucleotides incorporation in the DNA duplex stability and pairing properties to its complementary strands. In order to understand the effect of integration of (S)-BuNA nucleotides in the DNA duplex, we investigated conformational studies by CD spectro-

Table 1 Oligonucleotides used in the study

Entry	Sequences ^a	Nucleotides
ON-1	4'-aaaaaaaaaaaaaA-3' BuNA(A) ₁₄ dA	15
ON-2	4'-ttttttttttttT-3' BuNA(T) ₁₄ dT	15
ON-3	4'-aaaaaaaaaattttT-3'	16
ON-4	4'-atatatatatatA-3'	16
ON-5	5'-AAAAAAAAAAAAAAAAA-3'	15
ON-6	5'-AAAAAAAAAAAAAAAAA-3'	15
ON-7	5'-TTTTTTTTTTTTTTT-3'	15
ON-8	5'-TTTTTTTTTTTTTTT-3'	15

^a Lower case letters represent (S)-BuNA nucleotides and upper case letters represent DNA nucleotides. Sequences for BuNA are shown from 4' to 3' instead of 4' to 2' because BuNA oligonucleotides were synthesized on dA and dT CPG-solid supports.

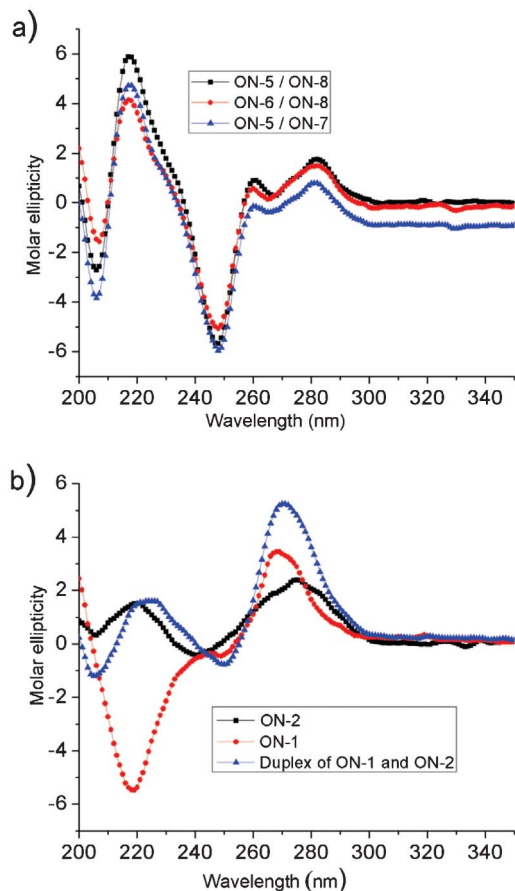


Fig. 2 CD profile of modified DNA duplexes and pairing of (*S*)-BuNA duplex. (a) Change in structural conformation by BuNA modified DNA strands (5 μ M each strand). (b) CD spectra of a 1 : 1 (5 μ M each strand) mixture of BuNA strands (ON-1 and ON-2) and individual strands ON-1 and ON-2 (20 μ M each). Experimental conditions: 10 mM phosphate buffer, 150 mM NaCl, pH 7.0 at 20 $^{\circ}$ C.

scopy and duplex stability by UV-melting. Two modified DNA strands ON-6 and ON-7 were studied, where a BuNA nucleotide was incorporated in the centre, since at this position maximum destabilization can be observed for the acyclic nucleotides.²⁴ UV-melting experiment at 260 nm revealed that integration of adenine (*S*)-BuNA nucleotide decreases the melting temperature (T_m) by 6 $^{\circ}$ C per modification, while incorporation of thymine nucleotide destabilizes the duplex by 9 $^{\circ}$ C.²³ Furthermore, CD studies revealed that these duplexes (ON-6/ON-8 and ON-5/ON-7) adopt a B-form structure, similar to the unmodified DNA duplex (ON-5/ON-8), which clearly indicates that integration of (*S*)-BuNA nucleotide does not affect the B-form structural conformation of DNA duplex (Fig. 2a).

In order to investigate the switching properties of a poly BuNA (A), it is important to understand the properties of individual strands of poly BuNA(A) and poly BuNA(T). At 20 $^{\circ}$ C a pentadecamer BuNA(A)₁₄dA (Table 1, ON-1) formed a left handed double helical structure with its complementary pentadecamer strand BuNA(T)₁₄dT (Table 1, ON-2) in 10 mM phosphate buffer containing 150 mM sodium chloride at pH

7.²³ Fig. 2b clearly indicates that the conformation of ON-1 is associated with a positive cotton effect at 269 nm and a negative cotton effect at 217 nm with a crossover at 247 nm, which revealed its preorganized structure. On the other hand, under similar experimental conditions, the CD of ON-2 showed positive peaks at 273 nm and 219 nm, and a negative peak at 242 nm with less cotton effect. The CD profile of the 1 : 1 mixture of ON-1 and ON-2 suggests a new conformation adopted by the duplex resulting in positive peaks at 273 nm and 217 nm with negative peaks at 245 nm and 203 nm (Fig. 2b). UV-melting at 260 nm was carried out to determine the T_m of the duplex (ON-1/ON-2), which was observed as 22 $^{\circ}$ C in 10 mM phosphate buffer in 1 M sodium chloride at pH 7 (data not shown). We were not surprised by the low duplex stability of ON-1 and ON-2 due to the unusual behaviour of poly (A) and poly (T).²⁵ To further demonstrate its pairing properties we analysed the duplex stability of self-complementary sequences ON-3 and ON-4, which showed melting temperatures of 39 $^{\circ}$ C and 40 $^{\circ}$ C, respectively, in 150 mM sodium chloride (data not shown). Based on literature evidence it can be suggested that (*S*)-BuNA adopts a left handed A-form-like structure.²⁶ These studies indicate that BuNA nucleotides do not alter the B-form of DNA duplexes and that BuNA oligonucleotides are capable of forming duplexes with their complementary strands.

pH-induced structural changes of ON-1 probed by CD (switching property)

The pH-induced structural transition of (*S*)-BuNA was investigated by CD. At neutral pH a positive cotton effect at 268 nm and a negative cotton effect at 217 nm were observed for ON-1 (Fig. 3a). The melting transition observed at pH 7.0 was found to be noncooperative (Fig. 3a inset).

These results suggest that at neutral pH, ON-1 demonstrates a weakly organized structure. On the other hand at pH 3.0 in unbuffered solution, ON-1 exhibited a more organized structure, which is supported by CD observation (Fig. 3b). A more profound peak with an increase in ellipticity up to six-fold at 265 nm with a blue shift from 268 nm, along with a shoulder peak at 273 nm was observed. Interestingly, the negative cotton effect at 217 nm (neutral pH) completely disappeared and a more prominent positive band at 217 nm emerged. It is evident from Fig. 3b (inset) that the melting transition is of cooperative nature at low pH, indicating a more rigid structure for ON-1. ON-3 also showed similar conformational changes at low pH, but the secondary structure was found to be less stable (Fig. S6, ESI[†]). These observations clearly indicate that a contiguous stretch of adenine nucleotides of BuNA undergoes conformational changes at low pH, which is termed as an A-motif.

Determination of apparent pK_a of A-motif

In order to understand the formation of the A-motif, it is important to determine its apparent pK_a .²⁷ At 20 $^{\circ}$ C a decrease in ellipticity at 265 nm was observed with increasing pH, with a sharp transition point at pH 4.8 in a citrate buffer, which indicates the two state transition of the A-motif (Fig. 4). The change in ellipticity at wavelength 265 nm was plotted as a function of pH, which revealed the existence of highly stable

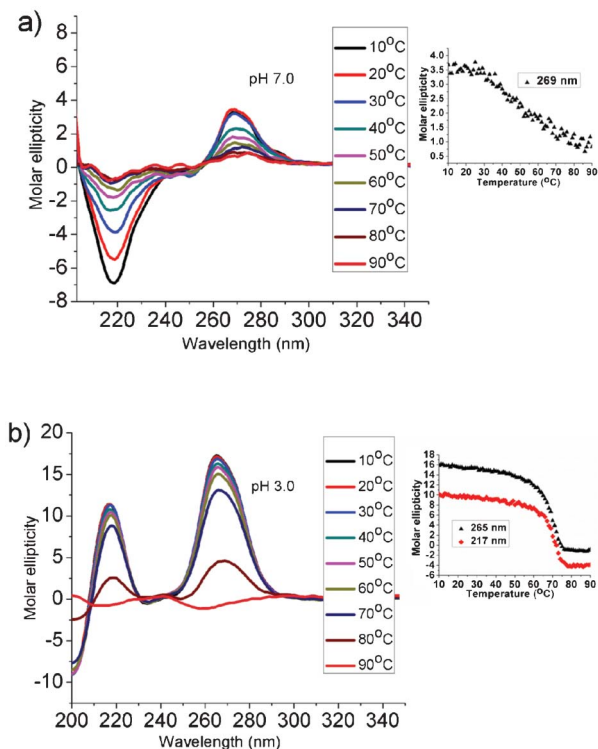


Fig. 3 Temperature-dependent CD profile of ON-1. (a) ON-1 with 20 μM oligonucleotide concentration in 10 mM phosphate buffer, 150 mM NaCl at pH 7. (b) ON-1 with 10 μM oligonucleotide concentration at pH 3. Insets: CD-melting profile of ON-1 at particular pH.

conformation in the range of pH (3 to 4.2). When the pH of the solution was increased (pH > 4.2), a gradual conversion of the rigid structure into a weakly organized one was observed (Fig. 4 inset). These observations clearly indicate that an A-motif exists at pH < 4.8, which dissociates into a single strand at pH > 4.8.

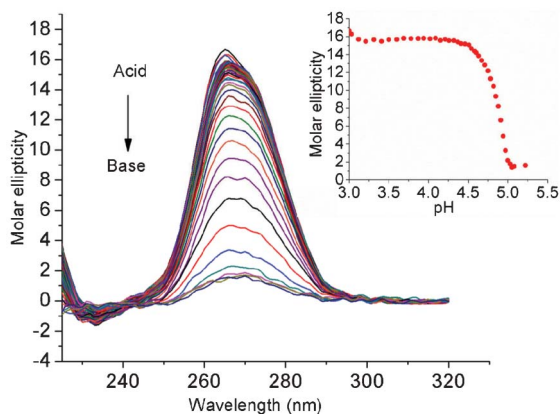


Fig. 4 pH-titration of 1 μM (ON-1) in 2 mM citrate buffer. Titration was started at pH 3.0 and pH was increased by gradual addition of sodium citrate. Inset shows the decrease in ellipticity at 265 nm on increasing pH of the solution. The midpoint pH of the transition results an apparent pK_a of the A-motif.

To prove the sequence dependency of the BuNA-based A-motif, similar experiments were carried out using ON-3. The conformational changes of ON-3 under acidic pH was easily affected by a slight increase in pH unlike ON-1, hence it was difficult to determine apparent pK_a for ON-3. In order to demonstrate the switching property of the A-motif, ON-1 was treated with alternating acid-basic cycles demonstrating it to be highly reversible (Fig. S7, ESI[†]). It is important to note that no precipitation was observed for ON-1 or ON-3 at pH 2.

Effect of salt on A-motif

The A-motif is stabilized by hydrogen bonds and salt bridges therefore, it is important to investigate the effect of strong electrolytes on its structure. It has been reported that the DNA-based A-motif is affected by the concentration of sodium chloride in the system, which was investigated by CD studies.^{21a} On similar lines, we investigated the effect of sodium chloride on the BuNA-based A-motif (ON-1). A solution of 1 μM oligonucleotide (ON-1) at pH 3.0 was treated with increasing sodium chloride concentrations resulting in a range from 0 mM to the 531 mM final concentration. CD was recorded after each addition, but the ellipticity at 217 nm

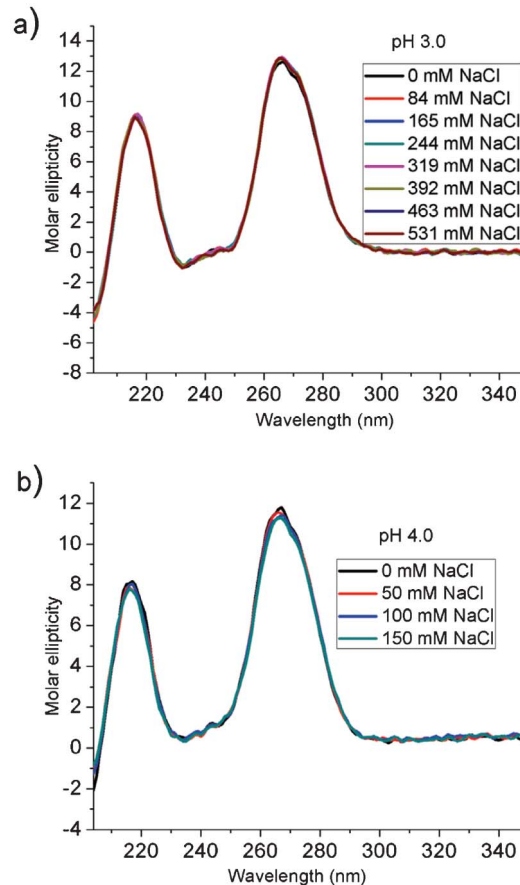


Fig. 5 Effect of sodium chloride on the A-motif (ON-1). (a) CD spectrum of ON-1 with 1 μM solution of oligonucleotide at pH 3.0 in unbuffered solution with different concentrations of sodium chloride. (b) Effect of sodium chloride in 10 mM acetate buffer at pH 4.

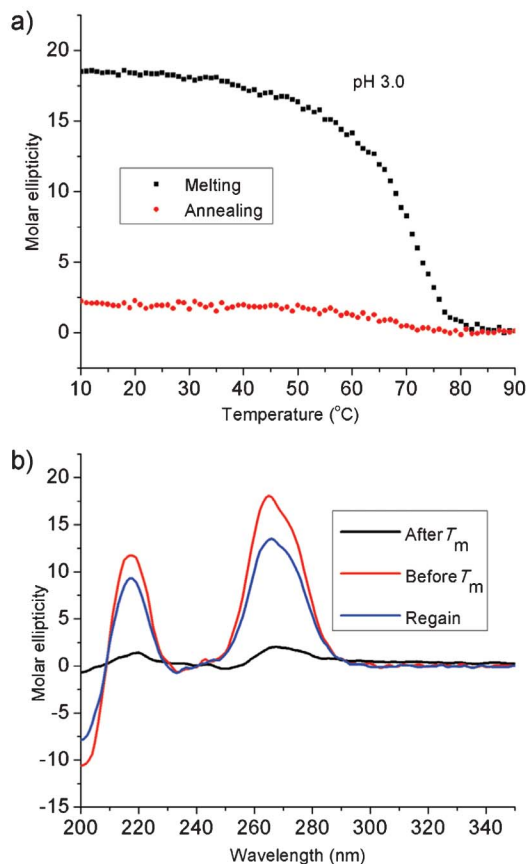


Fig. 6 Irreversibility of thermal melting transition of the A-motif (ON-1 with 1 μM oligo concentration). (a) CD-melting monitored at wavelength 265 nm in unbuffered aqueous solution at pH 3. (b) The CD signal was regained by addition of 0.1 N sodium hydroxide solution to neutralize the oligonucleotide solution followed by addition of 0.1 N hydrochloric acid to decrease the pH.

and 265 nm remained unchanged in the tested concentration range as evident from Fig. 5a.

A similar experiment was carried out in 10 mM sodium acetate buffer at pH 4.0, but no change in conformation was detected (Fig. 5b). These results clearly suggest that sodium chloride does not affect the structure of the BuNA-based A-motif.

Thermal stability of A-motif (ON-1) and effect of pH on reversibility of melting transition

We have demonstrated that at $\text{pH} > 4.8$ the BuNA-based A-motif exhibits a transition from highly organized to weakly organized structure. To study the thermal stability of the A-motif, melting studies were carried out in a pH range of 3 to 5. The melting temperature (T_m) value of ON-1 was determined to be 70 $^\circ\text{C}$ at pH 3.0 in unbuffered solution (Fig. 6a). Thermal transition was found to be irreversible at this pH. While determining T_m , it was noticed that the oligonucleotide solution became turbid and the intensity of CD signal was almost zero after the cooling ramp. Interestingly, the CD signal could be restored by increasing the pH of the turbid solution followed by acidification to the desired pH.

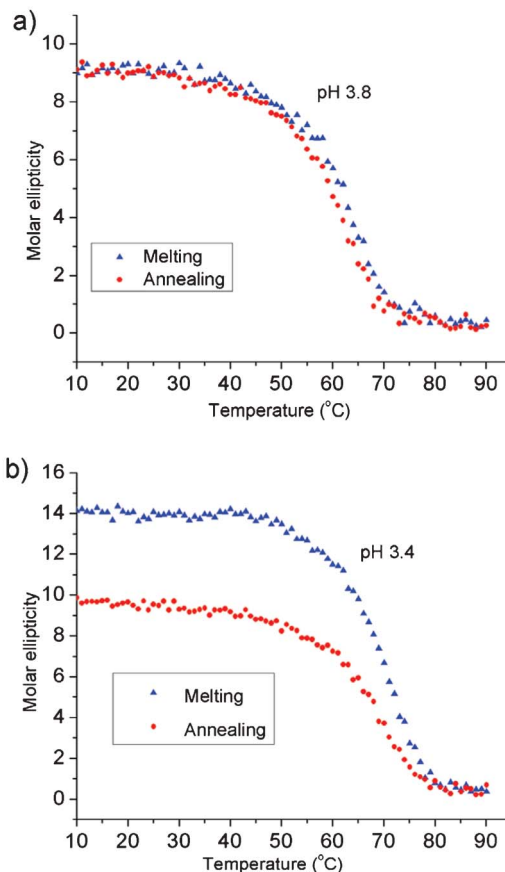


Fig. 7 Reversible CD-melting profile of A-motif (ON-1 with 1 μM oligo concentration) in 10 mM citrate buffer, monitored at wavelength 265 nm.

It is evident from Fig. 6b, that ON-1 regained its CD signal, whereas in the case of DNA no such observations were made. In order to achieve the reversible melting transition, a melting experiment at pH 3.8 was performed, where half of the adenine nucleotides were expected to be protonated. It is clear from Fig. 7a that the melting curve is completely reversible at pH 3.8 with a T_m of 64 $^\circ\text{C}$. After lowering the pH to 3.4 in citrate buffer, partial reversibility of the melting curve was observed with an increase in T_m to 73 $^\circ\text{C}$ (Fig. 7b). It is important to note that folding and unfolding of the A-motif at $\text{pH} > 3.8$ was completely reversible. These findings suggest that the A-motif displays a reversible melting transition at half or less than half protonation, while it exhibits an irreversible melting transition at more than half protonation of BuNA(A)₁₄dA. pH-dependent melting experiments show that the melting temperature increases with decreasing pH of the solution (Fig. 8a) (Table 2).

Furthermore, we investigated the effect of oligonucleotide concentration on melting temperature. T_m was determined with different concentrations of ON-1 (500 nM, 5 μM and 10 μM) at pH 4 in acetate buffer. It is evident from Fig. 8b that the melting temperature is concentration dependent. This study suggests that the A-motif is composed of intermolecular interactions between oligonucleotide strands.

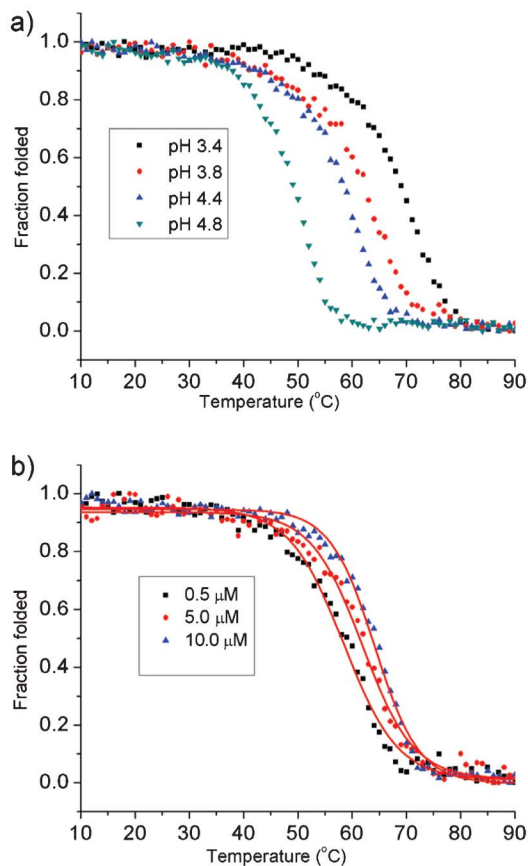


Fig. 8 Effect of pH and oligonucleotide concentrations on melting temperature of A-motif (ON-1). (a) pH-dependent melting experiment. All the melting profiles were generated at 265 nm with 1 μ M of ON-1 in 10 mM citrate buffer with different pH values. (b) Concentration dependent melting temperature in acetate buffer at pH 4. $T_m = 59$ $^{\circ}$ C (0.5 μ M); $T_m = 61$ $^{\circ}$ C (5 μ M); $T_m = 64$ $^{\circ}$ C (10 μ M). Solid lines represent sigmoidal curve fitting of melting curves.

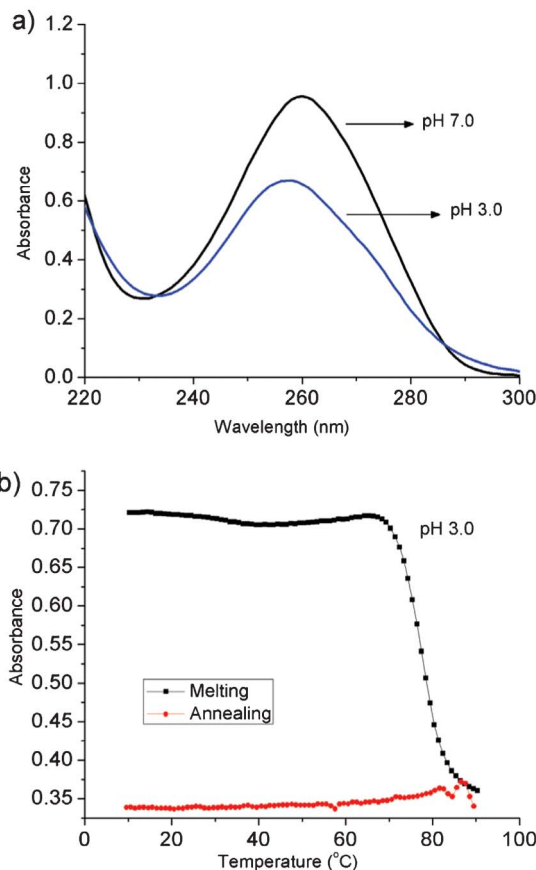


Fig. 9 (a) UV-spectrum of ON-1. (b) UV-melting profile at 260 nm of ON-1. Experiments were carried out in unbuffered solution with 4 μ M oligonucleotide solution at pH 3.

UV spectroscopy

Ultra-violet (UV) light absorption spectroscopy is sensitive to the stacking of π -bonded moieties such as nucleobases and to hydrogen bonding between nucleotides of nucleic acids. Therefore, it is an effective method to monitor the helix-to-coil transition between the folded and unfolded structure. UV spectral studies at neutral and acidic pH can provide structural insights into the BuNA-based A-motif. At 25 $^{\circ}$ C ON-1 was dissolved in 10 mM phosphate buffer at pH 7.0 showed a peak at 260 nm (Fig. 9a). On the other hand, in unbuffered aqueous solution at pH 3.0 a hypochromic effect was observed with a

blue shift at 258 nm (Fig. 9a). This hypochromic effect suggests that in acidic condition, ON-1 is a rigid structure compared to neutral pH. The T_m value of the A-motif was determined to be 77 $^{\circ}$ C in unbuffered solution at pH 3.0 (Fig. 9b). Melting curves clearly indicate a hypochromic effect at pH 3 instead of a hyperchromic one due to the turbidity of the solution. These results are in agreement with the observation made by CD-melting studies at pH 3. It is noteworthy that the UV-melting at pH 4 in acetate buffer was observed as reversible melting transitions with hyperchromic effect (data not shown). This study supports the reversible thermal melting transition of A-motif at pH > 3.8 which was investigated by CD-melting experiments. Similar UV-melting experiments were carried out with d(A)₁₅ (ON-5) at pH 3.0 with T_m (51 $^{\circ}$ C), where the melting curve can be easily differentiated from the depurination curve (Fig. S8, ESI†).

Table 2 Melting temperature of A-motif (ON-1) at different pH

Entry	pH	T_m ($^{\circ}$ C) ^a
1	3.4	73
2	3.8	64
3	4.4	59
4	4.8	49

^a Experiments were carried out in 10 mM citrate buffer.

MALDI-TOF-MS study of ON-1

Mass spectrometry (MS) has been proved as a successful technique to investigate non-covalent intermolecular interactions of DNA,²⁸ RNA²⁹ and DNA-RNA based molecular devices. MALDI-TOF-MS was used to further characterize BuNA based A-motif. Five peaks were observed at m/z [4243.692], [4243.692 + Na⁺], [4243.692 + K⁺], [4243.692 + Na⁺ + K⁺], and [4243.692 + 2

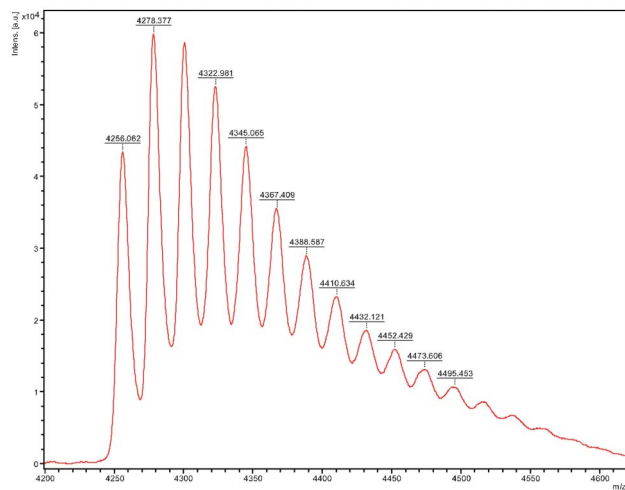


Fig. 10 MALDI-TOF-MS spectra of ON-1 (single strand).

K^+] at neutral pH, where the first peak corresponds to molecular weight of the ON-1 (Fig. S9a, ESI[†]). Next we investigated MALDI-TOF-MS of ON-1 in citrate buffer at pH 3. It is evident from Fig. 10 that a peak at m/z [4256.062] indicates $[MW + 12H^+]$ which corresponds to a protonated single strand. Formation of the A-motif was confirmed by interstrand interactions resulting in a peak at m/z [8513.225] corresponding to the duplex $[2MW + 25H^+]$ (Fig. 11). Other peaks observed in the mass spectrum belong to sodium adducts. These results clearly suggest that the A-motif is formed by two strands of ON-1.

Switching property of ON-3

We have demonstrated that a contiguous stretch of (*S*)-BuNA adenine nucleotides shows the pH-dependent behavior of an A-switch. To investigate the switching properties of a self-complementary strand of BuNA, an oligonucleotide containing a stretch of eight adenine nucleotides (ON-3) was used. CD

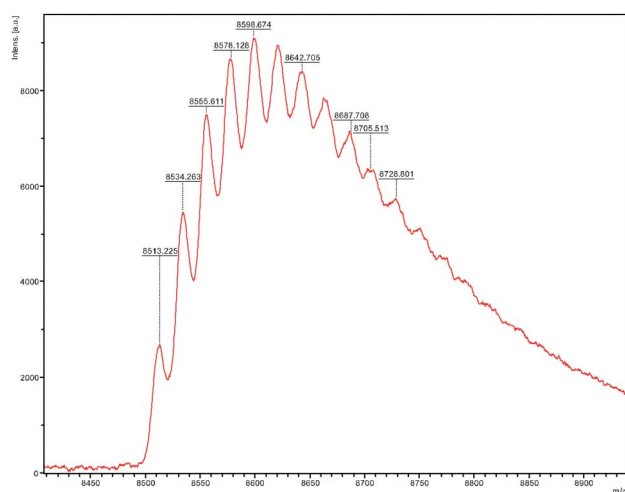


Fig. 11 MALDI-TOF-MS spectra of ON-1 (A-motif).

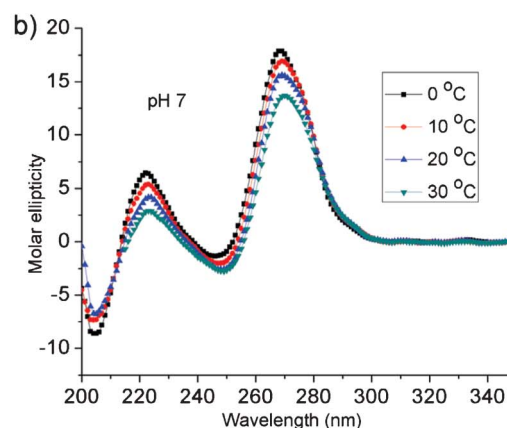
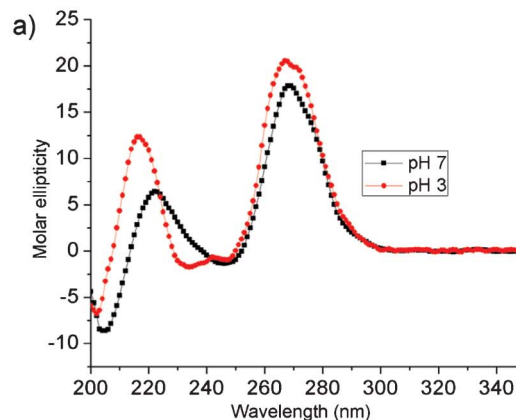


Fig. 12 (a) CD profile of ON-3 at pH 3 and pH 7 at 0 °C. (b) Temperature-dependent CD profile of ON-3 (4 μ M oligo concentration) in 10 mM tris-buffer containing 100 mM NaCl, 10 mM $MgCl_2$ at pH 7.

spectroscopy of ON-3 in 10 mM tris buffer containing 100 mM sodium chloride and 10 mM $MgCl_2$ at pH 7 revealed an A-form-like helical structure with positive ellipticity at 269 nm and 222 nm with negative peaks at 246 nm and 204 nm, (Fig. 12a). On the other hand, ON-3 under acidic condition adopted a different conformational structure, similar to A-motif (ON-1), with positive CD bands at 267 nm and 217 nm and a negative band at 234 nm (Fig. 12a). Fig. 12a demonstrates that the antiparallel duplex at neutral pH showed a positive ellipticity at 222 nm, while at low pH a positive peak with blue shift emerged at 217 nm with high intensity, which support the switching in conformation.

Temperature-dependent CD studies of ON-3 revealed stable duplex formation at pH 7 (Fig. 12b), while at low pH a decrease in stability was observed (Fig. 13a). In order to determine the stability of the A-motif of ON-3, CD-melting was carried out, which displayed a T_m of 12 °C (Fig. 13b). It is important to note that the melting transition of ON-3 was reversible at pH 3, which was observed to be irreversible for ON-1. At present we do not have experimental proof for the orientation of BuNA strands in the A-motif, which could be oriented in either parallel or antiparallel directions. Furthermore, ON-3 was analyzed by MALDI-TOF-MS. The mass spectrum shows a peak at m/z [4460.590] corresponding to a single strand $[MW + 3H^+]$

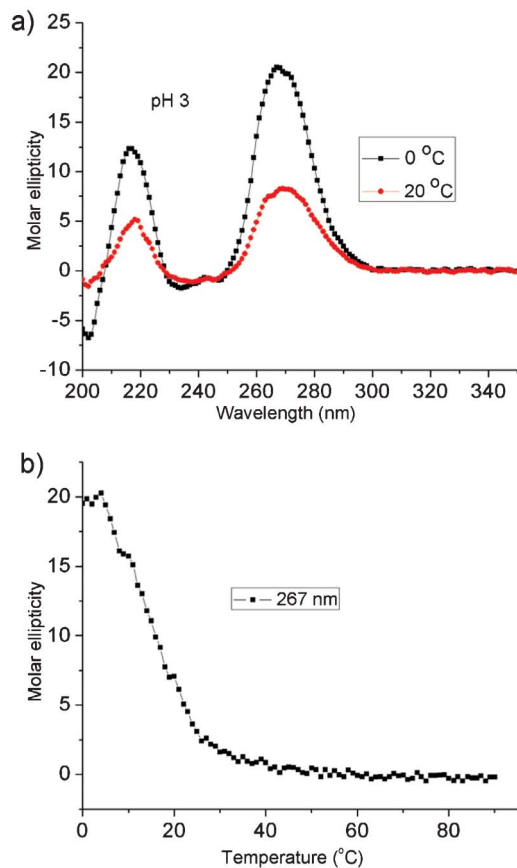


Fig. 13 (a) Temperature-dependent CD profile of ON-3 (4 μM oligo concentration) in 10 mM citrate buffer at pH 4. (b) CD-melting profile of ON-3 at pH 3.

(Fig. S9e, ESI†). At pH 3 a peak at m/z [4469.696] corresponds to $[\text{MW} + 9\text{H}^+]$ with six extra protons (Fig. S9g, ESI†) and the second peak at m/z [8936.886] corresponding to $[2\text{MW} + 15\text{H}^+]$ can be assigned to a duplex formation by two oligonucleotide strands (Fig. S9h, ESI†). Additionally, both the peaks are associated with sodium adducts as was observed for ON-1. These results clearly indicate the switching conformations of ON-3, from antiparallel duplex (pH 7) to A-motif, by the stimulus of protons.

Effect of flexible backbone of (S)-BuNA on A-motif

(S)-BuNA is composed of an acyclic backbone. Therefore one can debate that the formation of the A-motif might be due to backbone flexibility despite the contiguous stretch of acyclic adenine nucleotides. Therefore, we investigated other sequences (ON-2 and ON-4) to demonstrate the sequence-dependent formation of the A-motif. BuNA(T)₁₄dT (ON-2) failed to undergo such conformational changes (data not shown), since protonation and an A-form-like structure through the Hoogsteen hydrogen bonding is not possible for BuNA(T)₁₄dT under acidic condition. Next, we investigated the self-complementary BuNA sequence ON-4, where acyclic adenine and thymine nucleotides were arranged in an alternative fashion. In aqueous unbuffered solution at pH 3.0, ON-3 displayed no change in conformation (Fig. S10, ESI†).

These experiments prove that the switching property of ON-1 or ON-3 is not due to flexibility of the acyclic backbone, but due to the contiguous arrangement of BuNA adenine nucleotides. This study clearly indicates that polyadenine building blocks derived from either DNA or BuNA follow the same physical principles for formation of an A-motif.

Thermodynamics analysis of A-motif (ON-1)

The thermally-induced reversible melting transition of folded structures can be monitored by CD-melting.³⁰ Additionally, by selecting an appropriate wavelength, the decrease in ellipticity of CD with increasing temperature can be monitored, and converted to fraction folded *versus* temperature.³¹

Furthermore, this data can be used to obtain a Van't Hoff plot in order to determine thermodynamic parameters.³² The concentration-dependent melting temperature of ON-1 revealed the intermolecular nature of A-motif. Moreover, on the basis of MALDI-TOF-MS, a molecularity of two was used for calculating the thermodynamic parameters of A-motif. Free energy (ΔG°) of the A-motif (ON-1) was evaluated, where enthalpy and entropy are assumed to be independent of temperature using Gibbs equation $\Delta G^\circ = -RT \ln(K_a)$. K_a is the equilibrium constant of folding and unfolding of the A-motif.

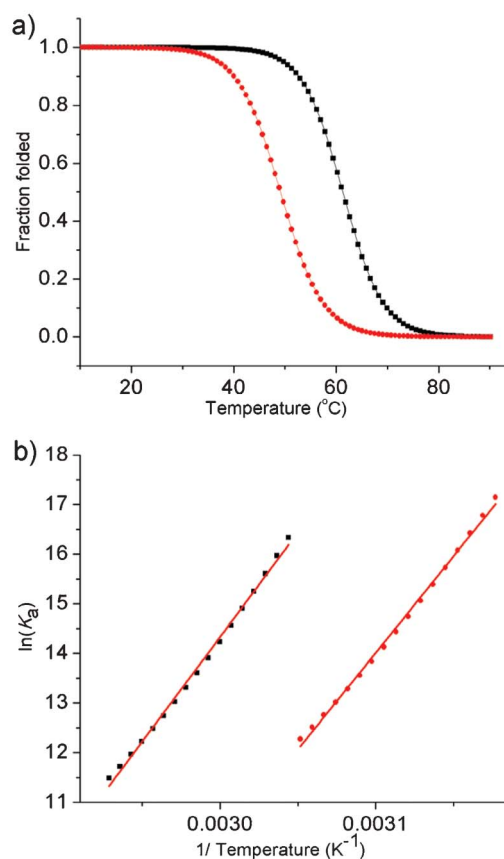


Fig. 14 Thermodynamic analysis of A-motif (ON-1) at pH 4.0 in 10 mM acetate buffer (squares: no salt was added, circles: 150 mM sodium chloride). (a) Fraction folded as a function of temperature. (b) Determination of ΔH° and ΔS° from Van't Hoff plot of $\ln(K)$ versus $1/T$. ΔH° was calculated from slope of the curve and ΔS° was calculated from intercept of the curve.

Table 3 Thermodynamic data of ON-1

NaCl (mM)	ΔH° (kcal mol ⁻¹)	ΔS° (kcal mol ⁻¹ K ⁻¹)	ΔG° (kcal mol ⁻¹)	T_m (°C)
0.0	-83.7	-0.222	-14.8	61
150	-75.6	-0.206	-11.7	48

CD-melting was carried out for ON-1 (1 μ M) in 10 mM of acetate buffer at pH 4 and heated from 10 °C to 90 °C at a heating rate of 1 °C min⁻¹ and the T_m value was determined to be 61 °C. It is noteworthy that no annealing is required for performing the melting experiment because the formation of the A-motif is an instantaneous process. The equilibrium constant was expressed as $K_a = \theta / (2c(1 - \theta)^2)$ for a bimolecular arrangement involving identical strands, where c is the total strand concentration and θ is the fraction of folded oligonucleotide, which was determined at each temperature from the reversible melting curve (Fig. 14a). To extract thermodynamic data we chose points with $0.15 \leq \theta \leq 0.85$ in the van't Hoff plot, because this is the region where K_a values are most precise.^{32b} In order to calculate enthalpy (ΔH°) and entropy (ΔS°) a plot of $\ln(K_a)$ against $1/T$ (K⁻¹) was plotted, which gave a straight line under a two-state transition model (Fig. 14b). The slope and intercept of the straight line correspond to $(-\Delta H^\circ/R)$ and $(\Delta S^\circ/R)$, respectively. Heating curves were corrected for baseline prior to evaluating the T_m and thermodynamic parameters (Table 3). Free energy (ΔG) was calculated at 37 °C.

In order to investigate the effect of sodium chloride on the thermal stability of the A-motif, similar experiments were carried out in the presence of 150 mM sodium chloride in acetate buffer at pH 4. The melting temperature was found to be 48 °C with free energy of folding $\Delta G^\circ = -11.7$ kcal mol⁻¹. These results clearly demonstrate that the presence of sodium chloride affects the thermal stability of the A-motif by destabilizing salt bridges. Since curve fitting (van't Hoff) analysis is only applicable for reversible melting transitions, determination of thermodynamic parameters of DNA-based A-motif was not possible due to the irreversible melting transition at pH 4.

Chemical integrity of A-motif

In order to investigate the chemical integrity of (*S*)-BuNA and DNA oligonucleotides at low pH, we performed stability tests. 10 μ M solution of each oligonucleotide in aqueous unbuffered solution at pH 3.0 was heated to 90 °C for 20 min. Analysis was carried out by reverse-phase HPLC by Luna C18 (100A, 250 \times 4.60 mm, 5 micron) column. A buffer system of 100 mM triethyl ammonium acetate at pH 7.0 with gradient flow (10–30% acetonitrile in 20 min) was used for eluting the oligonucleotides and its decomposed products. HPLC profiles (Fig. 15) demonstrate that BuNA nucleotides do not show depurination, while the DNA oligonucleotide (ON-5) decomposes, due to depurination of the deoxyadenine nucleotides. The HPLC chromatogram showed two peaks for ON-1 at 11.172 min and 10.185 min, which was expected due to the presence of one natural deoxyadenine nucleotide at the 3' end which underwent depurination (Fig. 15b). ON-3, which is composed of eight acyclic contiguous adenine nucleotides, did not show

any such decomposition, since no DNA adenine nucleotide is present in this sequence (Fig. S11b, ESI†). This clearly indicates that ON-5 was completely decomposed under acidic conditions at pH 3 (Fig. 15d), which showed a major peak at 4.144 min corresponding to adenine. This study suggests that the BuNA scaffold is chemically stable at low pH which is an important property for constructing molecular devices.

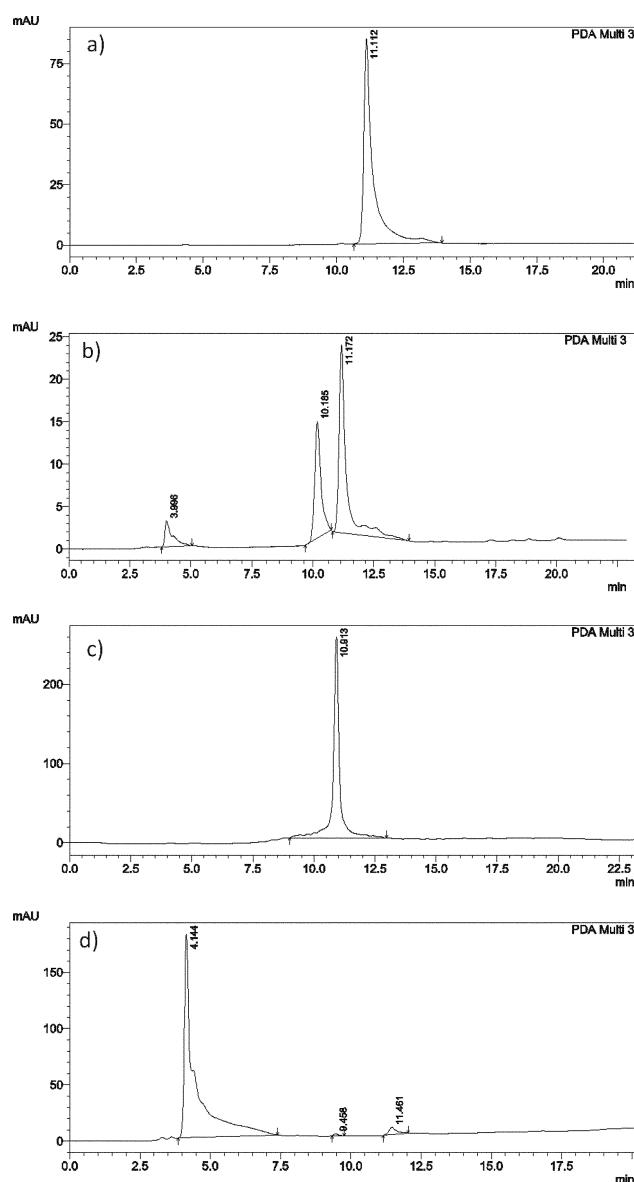


Fig. 15 HPLC profile of oligonucleotides. (a) ON-1. (b) ON-1 heated at pH 3. (c) ON-3. (d) ON-5 heated at pH 3.

Conclusions

In conclusion, we report the synthesis and construction of a BuNA-based A-switch. CD studies suggested that the (*S*)-BuNA duplex forms a left handed A-form-like structure at pH 7 and the incorporation of (*S*)-BuNA nucleotides does not alter the B-form helical structure of the DNA duplexes. UV and CD-melting studies revealed a highly stable structure of the A-motif. Furthermore, MALDI-TOF-MS experiments proved that the A-motif is assembled of two BuNA strands. Due to the chemical stability of BuNA at low pH, we were able to calculate thermodynamic parameters, where the ΔG value for the formation of the A-motif structure was determined to be $-14.8 \text{ kcal mol}^{-1}$ (pH 4.0, 37 °C). In the future these findings might provide a new platform for developing acyclic nucleic acids-based molecular devices. Further studies are going on to construct BuNA-based i-switches and G-quadruplexes.

Acknowledgements

The authors acknowledge financial support from the DBT and ICMR, Govt. of India (BT/PR/10064/AGR/36/30/07). The authors gratefully thank department of Chemistry IIT Madras, SAIF-IIT Madras for analytical data. Vipin thanks IIT Madras for fellowship. Vipin thanks to Prof. Yamuna Krishnan's research group from National Center for Biological Sciences (NCBS) India, for valuable discussion about DNA-based A-motif. Vipin thanks to Dr David Schaffert from Interdisciplinary Nanoscience Center-INANO-MBG, Aarhus University for proof reading of manuscript.

References

- (a) J. Bath and A. J. Turberfield, *Nat. Nanotechnol.*, 2007, **2**, 275–284; (b) M. M. Maye, M. T. Kumara, D. Nykypanchuk, W. B. Sherman and O. Gang, *Nat. Nanotechnol.*, 2009, **5**, 116–120; (c) A. Rajendran, M. Endo, Y. Katsuda, K. Hidaka and H. Sugiyama, *J. Am. Chem. Soc.*, 2011, **133**, 14488–14491; (d) A. V. Pinheiro, D. Han, W. M. Shih and H. Yan, *Nat. Nanotechnol.*, 2011, **6**, 763–772; (e) T. Topping, N. V. Voigt, J. Nangreave, H. Yan and K. V. Gothelf, *Chem. Soc. Rev.*, 2011, **40**, 5636–5646; (f) D. Ackermann and M. Famulok, *Nucleic Acids Res.*, 2013, **41**, 4729–4739.
- (a) K. Fukui, M. Morimoto, H. Segawa, K. Tanaka and T. Shimidzu, *Bioconjugate Chem.*, 1996, **7**, 349–355; (b) H. Asanuma, K. Shirasuka, T. Takarada, H. Kashida and M. Komiyama, *J. Am. Chem. Soc.*, 2003, **125**, 2217–2223.
- (a) P. Alberti, A. Bourdoncle, B. Sacca, L. Lacroix and J.-L. Mergny, *Org. Biomol. Chem.*, 2006, **4**, 3383–3391; (b) Y. Sannohe, M. Endo, Y. Katsuda, K. Hidaka and H. Sugiyama, *J. Am. Chem. Soc.*, 2010, **132**, 16311–16313; (c) A. Rajendran, S.-i. Nakano and N. Sugimoto, *Chem. Commun.*, 2010, **46**, 1299–1301; (d) Y. Krishnan and F. C. Simmel, *Angew. Chem., Int. Ed.*, 2011, **50**, 3124–3156; (e) J. Choi and T. Majima, *Chem. Soc. Rev.*, 2011, **40**, 5893–5909; (f) T. Li and M. Famulok, *J. Am. Chem. Soc.*, 2013, **135**, 1539–1599.
- (a) A. Pasternak and J. Wengel, *Bioorg. Med. Chem. Lett.*, 2011, **21**, 752–755; (b) T. B. Jensen, J. R. Henriksen, B. E. Rasmussen, L. M. Rasmussen, T. L. Andresen, J. Wengel and A. Pasternak, *Bioorg. Med. Chem.*, 2011, **19**, 4739–4745.
- N. Kumar, J. T. Nielsen, S. Maiti and M. Petersen, *Angew. Chem., Int. Ed.*, 2007, **46**, 9220–9222.
- (a) B. Datta, C. Schmitt and B. A. Armitage, *J. Am. Chem. Soc.*, 2003, **125**, 4111–4118; (b) B. Datta, M. E. Bier, S. Roy and B. A. Armitage, *J. Am. Chem. Soc.*, 2005, **127**, 4199–4207; (c) A. Paul, P. Sengupta, Y. Krishnan and S. Ladame, *Chem.-Eur. J.*, 2008, **14**, 8682–8689; (d) N. K. Sharma and K. N. Ganesh, *Chem. Commun.*, 2005, 4330–4332; (e) S. Modi, A. H. Wani and Y. Krishnan, *Nucleic Acids Res.*, 2006, **34**, 4354–4363.
- L. Lacroix and J.-L. Mergny, *Arch. Biochem. Biophys.*, 2000, **381**, 153–163.
- K. Kanaori, S. Sakamoto, H. Yoshida, P. Guga, W. Stec, K. Tajima and K. Makino, *Biochemistry*, 2004, **43**, 5672–5679.
- J. A. Brazier, J. Fisher and R. Cosstick, *Angew. Chem., Int. Ed.*, 2006, **45**, 114–117.
- (a) C. Mao, W. Sun, Z. Shen and N. C. Seeman, *Nature*, 1999, **397**, 144–146; (b) A. Rajendran, M. Endo, K. Hidaka and H. Sugiyama, *J. Am. Chem. Soc.*, 2013, **135**, 1117–1123.
- (a) S. A. Benner, *Science*, 2004, **306**, 625–626; (b) S. A. Benner, *Acc. Chem. Res.*, 2004, **37**, 784–797; (c) V. B. Pinheiro and P. Holliger, *Curr. Opin. Chem. Biol.*, 2012, **16**, 245–252.
- (a) K.-U. Schöning, P. Scholz, S. Guntha, X. Wu, R. Krishnamurthy and A. Eschenmoser, *Science*, 2000, **290**, 1347–1351; (b) V. B. Pinheiro, A. I. Taylor, C. Cozens, M. Abramov, M. Renders, S. Zhang, J. C. Chaput, J. Wengel, S.-Y. Peak-Chew, S. H. McLaughlin, P. Herdewijn and P. Holliger, *Science*, 2012, **336**, 341–344.
- (a) K. C. Schneider and S. A. Benner, *J. Am. Chem. Soc.*, 1990, **112**, 453–455; (b) Y. Merle, E. Bonnell, L. Merle, J. Sági and A. Szemző, *Int. J. Biol. Macromol.*, 1995, **17**, 239–246; (c) K. S. Ramasamy and W. Seifert, *Bioorg. Med. Chem. Lett.*, 1996, **6**, 1799–1804; (d) J. J. Chen, X. Cai and J. W. Szostak, *J. Am. Chem. Soc.*, 2009, **131**, 2119–2121; (e) E. Meggers and L. Zhang, *Acc. Chem. Res.*, 2010, **43**, 1092–1102; (f) P. Karri, V. Punna, K. Kim and R. Krishnamurthy, *Angew. Chem., Int. Ed.*, 2013, **52**, 5840–5844.
- (a) P. Nielsen, M. Egholm, R. Berg and O. Buchardt, *Science*, 1991, **254**, 1497–1500; (b) M. Egholm, O. Buchardt, L. Christensen, C. Behrens, S. M. Freier, D. A. Driver, R. H. Berg, S. K. Kim, B. Norden and P. E. Nielsen, *Nature*, 1993, **365**, 566–568.
- (a) P. Nielsen, L. H. Dreijøe and J. Wengel, *Bioorg. Med. Chem.*, 1995, **3**, 19–28; (b) H. Kashida, X. Liang and H. Asanuma, *Curr. Org. Chem.*, 2009, **13**, 1065–1084.
- (a) L. Zhang, A. Peritz and E. Meggers, *J. Am. Chem. Soc.*, 2005, **127**, 4174–4175; (b) R. S. Zhang, E. O. McCullum and J. C. Chaput, *J. Am. Chem. Soc.*, 2008, **130**, 5846–5847.
- (a) H. Asanuma, T. Toda, K. Murayama, X. Liang and H. Kashida, *J. Am. Chem. Soc.*, 2010, **132**, 14702–14703; (b) H. Kashida, K. Murayama, T. Toda and H. Asanuma, *Angew. Chem., Int. Ed.*, 2011, **50**, 1285–1288.
- (a) H. Asanuma, M. Akahane, N. Kondo, T. Osawa, T. Kato and H. Kashida, *Chem. Sci.*, 2012, **3**, 3165–3169; (b) T. Kato,

- H. Kashida, H. Kishida, H. Yada, H. Okamoto and H. Asanuma, *J. Am. Chem. Soc.*, 2013, **135**, 741–750.
- 19 J. R. Fresco and E. Klemperer, *Ann. N. Y. Acad. Sci.*, 1959, **81**, 730–741.
- 20 A. Rich, D. R. Davies, F. H. C. Crick and J. D. Watson, *J. Mol. Biol.*, 1961, **3**, 71–86.
- 21 (a) S. Chakraborty, S. Sharma, P. K. Maiti and Y. Krishnan, *Nucleic Acids Res.*, 2009, **37**, 2810–2817; (b) S. Saha, D. Bhatia and Y. Krishnan, *Small*, 2010, **6**, 1288–1292; (c) S. Kim, J. Choi and T. Majima, *J. Phys. Chem.*, 2011, **115**, 15399–15405; (d) S. Saha, K. Chakraborty and Y. Krishnan, *Chem. Commun.*, 2012, **48**, 2513–2515.
- 22 (a) D. Barszcz and D. Shugar, *Eur. J. Biochem.*, 1968, **5**, 91–100; (b) J. A. Zoltewicz, D. F. Clark, T. W. Sharpless and G. Grahe, *J. Am. Chem. Soc.*, 1970, **92**, 1741–1750; (c) A. I. S. Holm, L. Munksgaard Nielsen, S. Vronning Hoffmann and S. Brøndsted Nielsen, *Biopolymers*, 2012, **97**, 550–557.
- 23 V. Kumar, K. R. Gore, P. I. Pradeepkumar and K. Venkitasamy, *Org. Biomol. Chem.*, 2013, **11**, 5853–5865.
- 24 A. Pasternak and J. Wengel, *Nucleic Acids Res.*, 2010, **38**, 6697–6706.
- 25 (a) L. Peng and H.-J. Roth, *Helv. Chim. Acta*, 1997, **80**, 1494–1512; (b) K.-U. Schöning, P. Scholz, X. Wu, S. Guntha, G. Delgado, R. Krishnamurthy and A. Eschenmoser, *Helv. Chim. Acta*, 2002, **85**, 4111–4153.
- 26 (a) S. Sforza, G. Haaima, R. Marchelli and P. E. Nielsen, *Eur. J. Org. Chem.*, 1999, 197–204; (b) T. Tedeschi, S. Sforza, A. Dossena, R. Corradini and R. Marchelli, *Chirality*, 2005, **17**, S196–S204; (c) M. K. Schlegel, L.-O. Essen and E. Meggers, *Chem. Commun.*, 2010, **46**, 1094–1096.
- 27 A. J. Adler, L. Grossman and G. D. Fasman, *Biochemistry*, 1969, **8**, 3846–3859.
- 28 A. A. Stomakhin, V. A. Vasiliskov, E. Timofeev, D. Schulga, R. J. Cotter and A. D. Mirzabekov, *Nucleic Acids Res.*, 2000, **28**, 1193–1198.
- 29 Y. Xu, K. Kaminaga and M. Komiyama, *J. Am. Chem. Soc.*, 2008, **130**, 11179–11184.
- 30 N. J. Greenfield, *Nat. Protoc.*, 2007, **1**, 2527–2535.
- 31 D. Liu and S. Balasubramanian, *Angew. Chem., Int. Ed.*, 2003, **42**, 5734–5736.
- 32 (a) L. A. Marky and K. J. Breslauer, *Biopolymers*, 1987, **26**, 1601–1620; (b) J. D. Puglisi and I. Tinoco Jr, *Methods Enzymol.*, 1989, **180**, 304–325.